

Dynamical spatial-pattern memory in globally coupled lasers

Kenju Otsuka and Jyh-Long Chern

NTT Basic Research Laboratories, Musashino-shi, Tokyo 180, Japan

(Received 26 December 1991)

The chaotic dynamics found in globally coupled modulated laser systems have been switched into stable orbits, including antiphase periodic states and clustered states, by an injection-seeding method. Direct assignment to desired factorial periodic orbits has been demonstrated. Self-induced switching among destabilized clustered states (chaotic itinerancy) in the transition process from clustered states to global chaos has also been found.

PACS number(s): 42.50.Lc, 02.90.+p, 05.45.+b

Recently, applicability of high-dimensional complex dynamics to information storage (memory) has been investigated in nonlinear optical systems. Firth argued a fundamental relationship between *spatial chaos* and standard memory capacity in a simple model of cross-talking bistable optical pixels [1]. Rewritable *spatial chaos* memory has been proposed in a coupled optical bistable chain model by Otsuka and Ikeda [2]. Aida and Davis demonstrated experimentally that coexisting stable periodic *temporal* solutions due to complex bifurcation just before chaos in the optical bistable system with delay can be applied to ultrahigh-capacity dynamic memory [3]. On the other hand, Otsuka predicted numerically that $m_a = (N-1)!$ coexisting *dynamical spatial patterns*, i.e., antiphase periodic motions, can be selectively excited by applying seed signals to the modulated multimode lasers, where N is the number of oscillating modes, and succeeded in assignments to the antiphase dynamic spatial patterns up to $N=5$ ($m_a=24$) [4]. In this paper, we discuss the effect of the spontaneous-emission coefficient (noise) on stabilizing antiphase states in modulated multimode lasers. Also, the assignment to clustered states by "key pattern" injections and self-induced switching among destabilized clustered states (chaotic itinerancy [5]) are reported.

The governing equations for modulated multimode lasers with spatial hole burning are expressed as [4]

$$\frac{dn_0}{dt} = w_0 [1 + m \cos(\tau \omega_m t)] - n_0 - \sum_{l=1}^N (n_0 - n_l/2) s_l, \quad (1)$$

$$\frac{dn_k}{dt} = n_0 s_k - n_k \left[1 + \sum_{l=1}^N s_l \right], \quad (2)$$

$$\frac{ds_k}{dt} = K \{ [(n_0 - n_k/2) - 1] s_k + \epsilon_k n_0 + s_{i,k} \}, \quad (3)$$

$k = 1, 2, \dots, N,$

where $t = T/\tau$ is the normalized time (τ is population lifetime), w_0 is the normalized bias-pump power, m is the modulation depth, ω_m is the modulation frequency, n_0 is the dc component of the population density, n_k is the

first-order Fourier component of population density, s_k is the normalized photon density, $K = \tau/\tau_p$ (τ_p is photon lifetime), ϵ_k is the spontaneous-emission coefficient for the k th mode, and $s_{i,k}$ is an injection-seed signal. Here, we assume uniform effective gain for lasing modes for brevity. In this model, longitudinal modes are coupled globally through cross-saturation of population density resulting from the spatial hole burning.

From linear stability analysis, an N -mode free-running laser is found to be always stable in time, and the relaxation oscillation at $\omega_r = [(w-1)/\tau\tau_p]^{1/2}$ is damped out. If the modulation depth increases to where the pump power drops below the threshold during part of the pump modulation cycle, the total output behaves just like a single-mode laser and exhibits spiking-mode oscillations at $\omega_s < \omega_r$, while each emitter exhibits N -alternative spiking pulsations at ω_s/N , resulting from winner-takes-all dynamics based on the cross-saturation mechanism. This is manifested as the antiphase states in modulated multimode lasers [4]. For small N , the antiphase states are globally attracting and are obtained after short transients for arbitrary initial conditions. There coexist $m_a = (N-1)!$ antiphase stable periodic attractors in the phase space in such a case.

When N increases, the basin of attraction of antiphase states shrinks very rapidly and antiphase attractors tend to coexist with chaotic orbits in the phase space. In addition, p -clustered states appear, where oscillating modes are divided into p groups that exhibit different synchronized motions. There coexist at least $m_c = N!/N_1!N_2! \cdots N_p!$ clustered states in the phase space, where N_i is the number of modes belonging to the i th cluster. The bifurcation diagram for a five-mode laser is shown in Fig. 1(a) as a function of modulation frequency, where $w_0 = 2.7$, $m = 0.74$, $K = 1000$, and $\epsilon_k = 1.2 \times 10^{-7}$ are assumed. In the high-modulation-frequency side near ω_r , synchronized relaxation oscillations are realized. When the modulation frequency is decreased, clustered states like those in Fig. 1(b) appear. Figure 1(b) shows a two-cluster state [(1,2,3),(4,5)], where the amplitudes of the five modes ($k = 1, 2, 3, 4, 5$) are drawn in the figures in increasing order from bottom to top hereafter. It is interesting to note that the total output exhibits the alter-

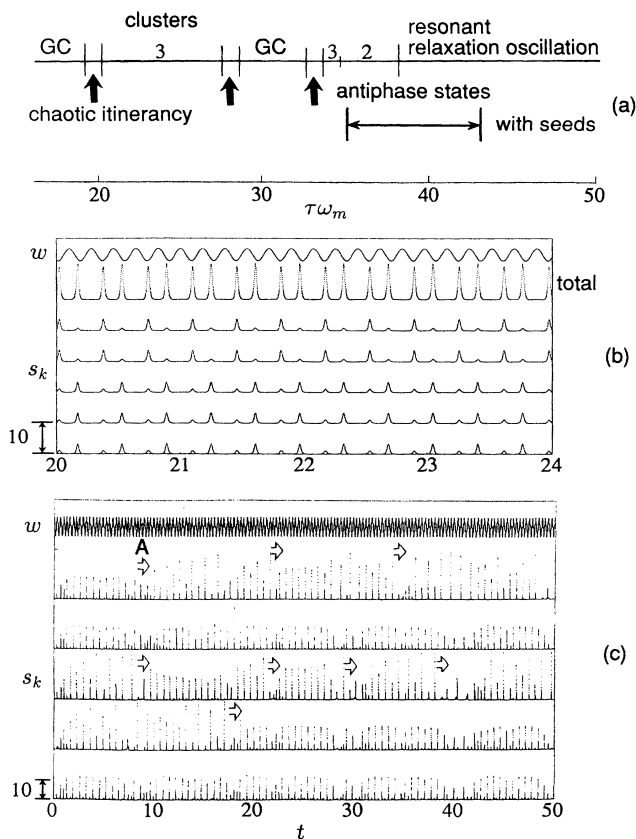


FIG. 1. (a) Bifurcation diagram for a five-mode laser. See the text for parameters. (b) Two-cluster state; $\tau\omega_m = 35$; (c) chaotic itinerancy; $\tau\omega_m = 19.5$.

native spike pulses of the spiking mode and the resonant relaxation oscillation, which was observed experimentally in a modulated *single mode* $\text{LiNdP}_4\text{O}_{12}$ (LNP) laser [6]. Indeed, the total output wave form has been found to coincide almost with the single-mode laser output wave form calculated by assuming $N = 1$ and the same parameter values [7]. This implies that dynamics of individual modes are self-organized such that the total output behaves just like a single-mode laser similar to antiphase states. It should be noted that these stable synchronized relaxation oscillations or stable clustered motions coexist both with the chaotic attractor and antiphase states with different basins of attraction in the phase space.

If the modulation frequency is decreased further, clustered states are destabilized and then the system exhibits self-induced switching among coexisting destabilized clustered motions (chaotic itinerancy [5]) leading to a global chaos (GC in Fig. 1). This process repeats when the modulation frequency is decreased as shown in the figure. Figure 1(c) shows an example of chaotic itinerancy at $\tau\omega_m = 19.5$, where at point A, for example, the switching from a destabilized [(1,4,5),2,3] cluster to a destabilized [(1,3,4),2,5] cluster is occurring.

The basin of attraction of antiphase states for $N = 5$ is extremely small in this parameter range, and it is hard for

the system to reach the basin of attraction. However, one can assign the system to the desired antiphase dynamics states by injecting small light pulses [\approx (laser pulse height)/60] to ($N - 1$) modes in the desired sequences as seeds at the time interval of $2\pi/\omega_s$ only during the ($N - 1$) modulation cycle in the region indicated in Fig. 1(a). Examples are shown in Fig. 2 for $\tau\omega_m = 35$. In Fig. 2(a) the system shows chaotic evolutions initially and is switched to the antiphase state by the seed pulses. In the case of Fig. 2(b) with slightly different initial conditions from Fig. 2(a), the system is attracted by the two-cluster state [(1,2,3,4),5] after some transients and is switched to the antiphase states by seed pulses. These results imply that chaotic, cluster, and antiphase attractors indeed coexist in the phase space for $\tau\omega_m = 35$, and switching among them can be established by injection seeding. The seeding condition for realizing antiphase states in terms of pulse height and pulse width is not so severe when the seed pulses are applied to modes in synchronization with the pump maxima. Moreover, even switching from one antiphase state to another is possible [4].

Resonant relaxation oscillations or clustered states have larger basins of attraction than antiphase states and generally exist independently of the system size N . Indeed, they are found to be realized when the chaotic orbit collides with the orbit of synchronized relaxation oscillation or clustered state (crisis [8]) in the temporal-evolution process. However, in the case of clustered states, which clustered state is realized critically depends on initial conditions. If one can assign the system to a

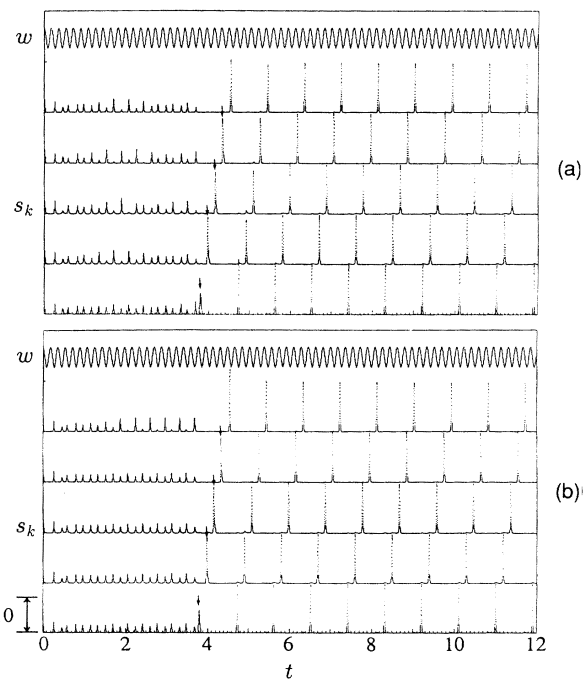


FIG. 2. Assignment to antiphase states. Parameter values are the same as for Fig. 1. $\tau\omega_m = 35$, seed pulse height = 0.2, and pulse width = 0.06. (a) Switching from chaotic orbit to antiphase state. (b) Switching from clustered state to antiphase state.

desired clustered state, a dynamic pattern memory with a large capacity is expected. From the numerical simulations, it is found that direct assignment to the desired clustered states is possible when key patterns of the desired clustered states are applied to some modes as seeds in the first modulation cycle. Examples are shown in Fig. 3 for $\tau\omega_m=25$. In Fig. 3(a) the system is initially in the chaotic attractor, and the chaotic dynamics are switched to a three-cluster state [(1,2,3),4,5] by applying key patterns to $k=1, 2$, and 3 modes, where seed pulse height $s_{k,i}$ ($k=1,2,3$) is 0.2 and pulse width is 0.06. In Fig. 3(b) the system is switched to a three-cluster state [(1,4,5),2,3] by applying key patterns to $k=2$ and 3 modes, where seed pulse heights are $s_{2,i}=0.2$ and $s_{3,i}=0.1$. Here, other modes are self-organized such that the total output behaves just like a single mode and exhibits alternative spike pulses similar to Fig. 1(b). In other words, the desired clustered state can be associatively memorized by injection seeding of key patterns during one modulation cycle. It is very likely that injection seeds give a driving force to the system such that the trajectory will fall on the basin of attraction of these periodic states surrounded by a chaotic sea through saddles (homoclinic crossing). Such an assignment process can be called *seeding-assisted crisis*.

The basin of attraction of antiphase states depends on the spontaneous emission coefficient ϵ_k . In general, if ϵ_k is decreased, the basin of attraction increases as a result of the reduction of fluctuations due to the $\epsilon_k n_0$ term in Eq. (3). For $\epsilon_k \geq 5 \times 10^{-8}$, antiphase attractors are destroyed for $N \geq 6$. In the case of $N=6$, antiphase attrac-

tors are divided into $N=5$ antiphase motions and the chaotic motion. However, the sequential playback of the forced $N=6$ antiphase motions, which do not exist previously in the phase space, can be accomplished by applying clock optical pulses to the first firing mode in addition to the injection seeds. The result is shown in Fig. 4(a), where the antiphase is destroyed into $N=5$ antiphase motions and chaotic motion when the clock pulse is cut. When the spontaneous emission coefficient ϵ_k is decreased, the basin of attraction of antiphase states increases; the $N=6$ antiphase states ($m_a=120$) have a finite basin of attraction for $\epsilon_k < 5 \times 10^{-8}$, and one can assign the system to these antiphase states without applying clock pulses, as shown in Fig. 4(b), where $\epsilon_k = 1.2 \times 10^{-8}$. If ϵ_k is decreased further to 1.2×10^{-9} , for example, which is an attainable value in solid-state lasers [6], sequential playback like that in Fig. 4(a) is possible even for $N=7$ (i.e., $m_a=720$). (Modification of the spontaneous-emission coefficient has been reported in a semiconductor material device [9]). The seeded-assignment method in the present system is attractive in terms of application to a memory of factorial dynamical spatial patterns resulting from automatic parallel processing among oscillating modes with cross-saturation. The memory capacity in the present system is expressed by $C_a = \log(N-1)!/\log 2$ for antiphase states and

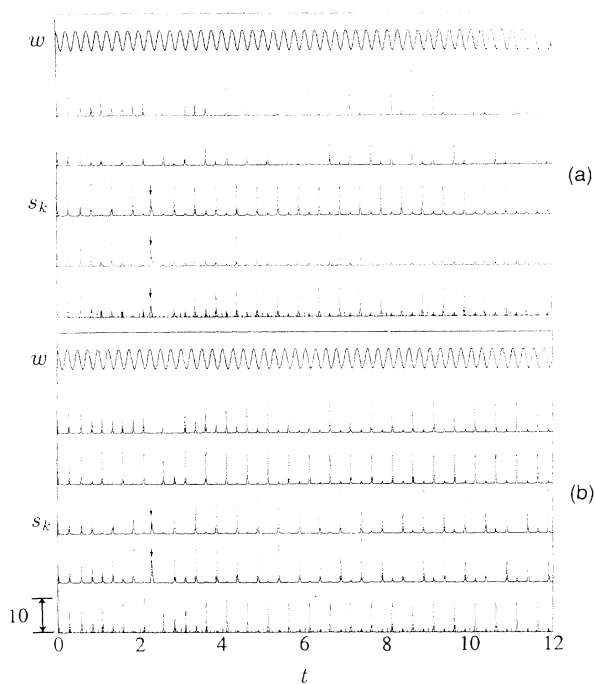


FIG. 3. Assignment to clustered states. Parameter values are the same as for Fig. 1; $\tau\omega_m=25$. (a) Seed pulses $s_{k,i}$ ($k=1,2,3$)=0.2 and pulse width = 0.06. (b) Seed pulses $s_{2,i}=0.2, s_{3,i}=0.1$ and pulse width = 0.06.

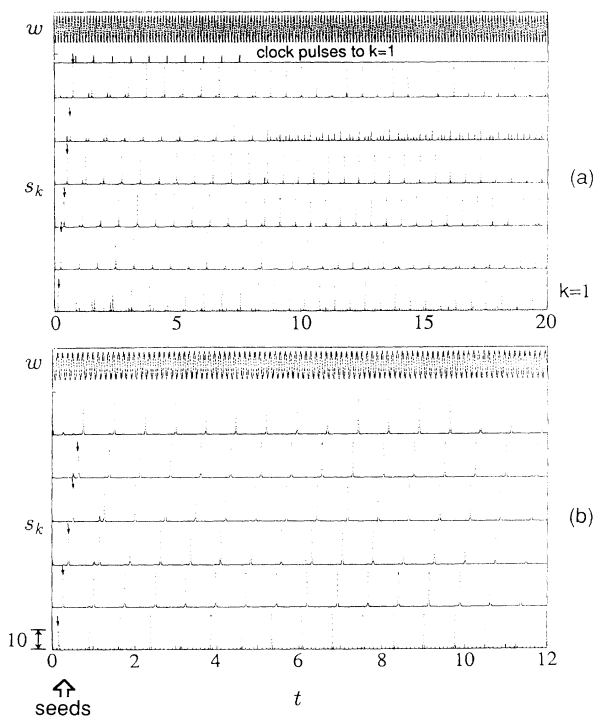


FIG. 4. (a) Sequential playback to forced antiphase states for $N=6$ with $\epsilon_k = 1.2 \times 10^{-7}$ by clock pulses. $w_0=4.2$, $m=0.76$, and $\tau\omega_m=51$. Seed pulse height = 0.2 and pulse width = 0.02. Clock pulse height = 0.2 and pulse width = 0.05. (b) Assignment to $N=6$ antiphase states for a decreased ϵ_k of 1.2×10^{-8} , where other parameter values are the same as (a).

$C_c = \log(N!/N_1!N_2! \cdots N_p!)/\log 2$ for p -cluster states. This implies that the memory capacity per mode exceeds ordinary one-bit binary memory.

Finally, the globally coupled laser array (GCLA), which exhibits exactly the same dynamics described so far for multimode lasers, is proposed as another example. In the conceptual model of the GCLA shown in Fig. 5, the output from single-mode laser emitters oscillating in the linear polarization (such as laser diodes, anisotropic lasers [6], and a laser with an intracavity Brewster plate) are passed through a traveling-wave amplifier and are combined by a multiport fiber coupler. The total output from the fiber is retroreflected into emitters through the Faraday rotator, analyzer, and mirror. In this scheme, the feedback light is polarized perpendicular with respect to the oscillating beam. Therefore, all the emitters are globally coupled by *incoherent* feedback [10]. In other words, the reflected beam acts as a cross-saturation beam for the population density in each emitter similar to multimode lasers. The amplifier is introduced to control the degree of cross-saturation. The dynamical equations are similar to Eqs. (1)–(3),

$$\frac{dn_k}{dt} = w_{0,k} [1 + m \cos(\omega_m)] - n_k \left[1 + s_k + (\gamma/N) \sum_{l=1}^N s_l(t-t_l) \right], \quad (4)$$

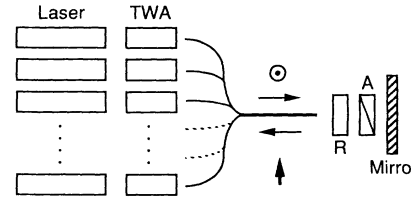


FIG. 5. Conceptual model of globally coupled laser arrays. TWA, traveling-wave amplifier; R, Faraday rotator; A, analyzer.

$$\frac{ds_k}{dt} = K [(n_k - 1)s_k + \epsilon_k n_k + s_{i,k}], \quad k = 1, 2, \dots, N, \quad (5)$$

where γ is the feedback coefficient which expresses the degree of cross-saturation. For a short delay, i.e., $t_l \ll 1$, exactly the same dynamics as described before for multimode lasers take place resulting from the common cross-saturation mechanism.

In conclusion, the direct assignment to antiphase as well as clustered states based on the injection-seeding method was demonstrated theoretically for deeply modulated multimode lasers. The sequential playback of previously nonexistent periodic orbits by clock pulses and the effect of the spontaneous-emission coefficient on the assignment procedure were discussed. Chaotic itinerancy among destabilized clustered states was found in the transition process from clustered states to global chaos.

[1] W. J. Firth, *Phys. Lett. A* **125**, 375 (1987).

[2] K. Otsuka and K. Ikeda, *Phys. Rev. A* **39**, 5209 (1989).

[3] T. Aida and P. Davis, in *Proceedings on the Topical Meeting on Nonlinear Dynamics in Optical Systems*, edited by N. B. Abraham, E. Garmire, and P. Mandel (The Optical Society of America, Washington, DC, 1990), p. 540.

[4] K. Otsuka, *Phys. Rev. Lett.* **67**, 1090 (1991).

[5] For a review, see K. Otsuka, *Int. J. Mod. Phys. B* **5**, 1179 (1991).

[6] K. Kubodera and K. Otsuka, *IEEE J. Quantum Electron.*

QE-17, 1139 (1981).

[7] If we introduce $S \equiv \sum_k s_k$ and $N \equiv \sum_k n_k$, Eqs. (1)–(3) are well approximated by the single-mode equation.

[8] C. Grebogi, E. Ott, and J. A. Yorke, *Physica D* **7**, 181 (1981).

[9] E. Yablonovitch, T. J. Gmitter, and R. Bath, *Phys. Rev. Lett.* **61**, 2546 (1988).

[10] H. Yasaka, Y. Yoshikuni, and H. Kawaguchi, *IEEE J. Quantum Electron.* **QE-27**, 193 (1991); K. Otsuka and J. -L. Chern, *Opt. Lett.* **16**, 1759 (1991).